The lysosomal polypeptide transporter TAPL is stabilized by interaction with LAMP-1 and LAMP-2

Özlem Demirel[1,*], Irina Jan[1,*], Dirk Wolters[2], Judith Blanz[3], Paul Saftig[3], Robert Tampé[1] and Rupert Abele[1,‡]

[1]Institute of Biochemistry, Biocenter, Goethe-University Frankfurt, Max-von-Laue-Str. 9, 60438 Frankfurt am Main, Germany
[2]Department of Analytical Chemistry, Ruhr-University Bochum, Universitaetsstr. 150, 44780 Bochum, Germany
[3]Biochemical Institute at the University Kiel, Olshausenstrasse 40, 24098 Kiel, Germany

*These authors contributed equally to this work
‡Author for correspondence (abele@em.uni-frankfurt.de)

Accepted 9 May 2012
Journal of Cell Science 125, 4230–4240

doi: 10.1242/jcs.087346

Summary

TAPL (ABCB9) is a homodimeric polypeptide translocation machinery which transports cytosolic peptides into the lumen of lysosomes for degradation. Since the function of proteins is strongly dependent on the interaction network involved, we investigated the interactome of TAPL. A proteomic approach allowed identification of the lysosome-associated membrane proteins LAMP-1 and LAMP-2B as the most abundant interaction partners. Albeit with low frequency, major histocompatibility complex II subunits were also detected. The interaction interface with LAMP was mapped to the four-transmembrane helices constituting the N-terminal domain of TAPL (TMD0). The LAMP proteins bind independently to TAPL. This interaction has influence on neither subcellular localization nor peptide transport activity. However, in LAMP-deficient cells, the half-life of TAPL is decreased by a factor of five, whereas another lysosomal membrane protein, LIMP-2, is not affected. Reduced stability of TAPL is caused by increased lysosomal degradation, indicating that LAMP proteins retain TAPL on the limiting membrane of endosomes and prevent its sorting to intraluminal vesicles.

Key words: ABC transporter, Lysosomal peptide translocation, Protein interaction, Subcellular trafficking, TMD0

Introduction

Lysosomes are single-membrane-bound organelles for degradation of endogenous or exogenous macromolecules. Therefore, lysosomes are filled with an armada of different hydrolases that function optimally at acidic pH. Mutations of these hydrolases are related to different storage disorders characterized by lysosomal accumulation of catabolic macromolecular intermediates influencing the cellular homeostasis (Ballabio and Gieselmann, 2009; Lübke et al., 2009). The lysosomal membrane comprises a unique set of membrane proteins fulfilling a broad spectrum of tasks (Bagshaw et al., 2005; Schröder et al., 2007). The proton motive force, generated by the V-type ATPase, drives the export of catabolites by membrane transporters into the cytosol for their biosynthetic reuse. Complex membrane bound protein machineries mediate the movement of lysosomes along microtubules for fusion and fission with target organelles like phagosomes, endosomes or autophagosomes for delivery of substrates. Additionally, macromolecules are provided by transport complexes into the lumen of lysosomes for their degradation (Saftig, 2005; Saftig and Klumperman, 2009).

Among the approx. 50 different lysosomal storage diseases, only a few are linked to membrane proteins (Lübke et al., 2009). Danon disease, characterized by hypertrophic cardiomyopathy, skeletal myopathy and variable mental retardation, is caused by mutations of the X-linked gene encoding for the lysosome-associated membrane protein type 2 (LAMP-2) (Nishino et al., 2000). A high proportion of mice deficient in LAMP-2 die shortly after birth and many tissues of these animals are characterized by an accumulation of autophagosomes (Tanaka et al., 2000). This type I transmembrane glycoprotein comprises a large, highly N- and O-glycosylated luminal domain, followed by a transmembrane helix and a short C-terminal, cytosolic domain (Eskelinen et al., 2005). Three splice isoforms of LAMP-2 (A, B, C) are found, which differ in the transmembrane helix and the cytosolic part encoded by exon 9 (Gough et al., 1995; Hatem et al., 1995). LAMP-2A is the putative receptor and transporter in chaperone mediated autophagy (Cuervo and Dice, 2000). Interestingly, deficiency in LAMP-1, which shows a sequence homology of 37% to LAMP-2, is tolerated by mice with only minor effects as reflected by mild astrogliosis and altered immunoreactivity against cathepsin D in the brain (Andrejewski et al., 1999).

Recently, the transporter associated with antigen processing like (TAPL) was deciphered as a lysosomal polypeptide import machinery (Demirel et al., 2007; Wolters et al., 2005; Zhang et al., 2000). Peptides of 6- to 59 amino acids in length, recognized via free N- and C-terminus as well as the N- and C-terminal residues, are transported with low affinity (Zhao et al., 2008). TAPL belongs to the ATP binding cassette (ABC) transporter family, which translocates a broad spectrum of solutes across cellular membranes powered by ATP hydrolysis. TAPL is a homodimeric transport complex (Leveson-Gower et al., 2004). Each subunit contains an N-terminal transmembrane domain and a C-terminal, cytosolic nucleotide binding domain (NBD). Functionally, TAPL can be dissected into TMD0, which shows no sequence homology to proteins in the data bases, and the core complex (Demirel et al., 2010). Core-TAPL, composed of the six putative C-terminal transmembrane helices and the NBD, is fully active in peptide transport but mistargeted predominantly to

Journal of Cell Science

the plasma membrane when expressed alone. TMD0, which comprises the four N-terminal putative transmembrane helices, encodes the targeting domain for lysosomal localization (Kamakura et al., 2008) and is able to redirect the core complex to lysosomes by non-covalent interactions (Demirel et al., 2010).

This lysosomal peptide transporter is found in different tissues, with strongest expression in testes (Zhang et al., 2000). However, it is also detected in other tissues like brain and spinal cord. On cellular level, TAPL is expressed in Sertoli and HeLa cells (Kobayashi et al., 2003; Zhang et al., 2000). Interestingly, a strong protein induction is observed in dendritic cells and macrophages during maturation implying an involvement of TAPL in antigen presentation. However, a role in the classical major histocompatibility complex class I dependent pathway was excluded (Demirel et al., 2007).

In the postgenomic era, a strong focus is set on the characterization of the interaction network of protein complexes, which is crucial for the understanding of the cellular function of proteins. Interaction partners can stabilize proteins, function as regulator, influence ligand affinity and specificity, escort the binding partner to distinct subcellular compartments or tether them to a specific environment. To identify the interactome of the lysosomal peptide transport complex TAPL, we have isolated TAPL by tandem affinity purification and determined interaction partners by two-dimensional liquid chromatography in combination with tandem mass spectrometry. After verification of the interaction partners on endogenous expression level, we could assign the interaction domain in TAPL. With the help of knock-out cells, the importance of the identified interactions on TAPL function was revealed.

Results

Functionality of TAPL variants containing a C-terminal tandem affinity purification tag

For identification of interaction partners of the lysosomal peptide transporter TAPL, a tandem affinity purification tag (tg) was attached to the C-terminus of wt-TAPL and core-TAPL. The tag comprised a calmodulin binding peptide followed by a tobacco etch virus (TEV) protease cleavage site and a C-terminal *Staphylococcus aureus* derived tandem protein A domain (Fig. 1A). Since tagged and untagged TAPL variants, stably expressed by retroviral transduction in the human B-lymphoma cell line Raji showed similar expression, we assumed correct folding of the proteins (Fig. 1B). Furthermore, the tandem affinity purification tag did not influence the subcellular localization. Full-length TAPL with (wt-TAPL-tg) or without the additional tag (wt-TAPL) trafficked exclusively to lysosomal compartment as reflected by a Pearson coefficient of nearly one. Therefore, wt-TAPL did not colocalize with the 58K Golgi protein (Golgi marker) nor with the cation independent mannose-6-phosphate receptor (late endosome marker) (supplementary material Fig. S1). The core complex displayed a more diffuse staining with preferential targeting to the plasma membrane and only marginal colocalization with the lysosomal marker LAMP-2 (Pearson coefficient 0.24 to 0.33) (Fig. 1C). The diffuse intracellular

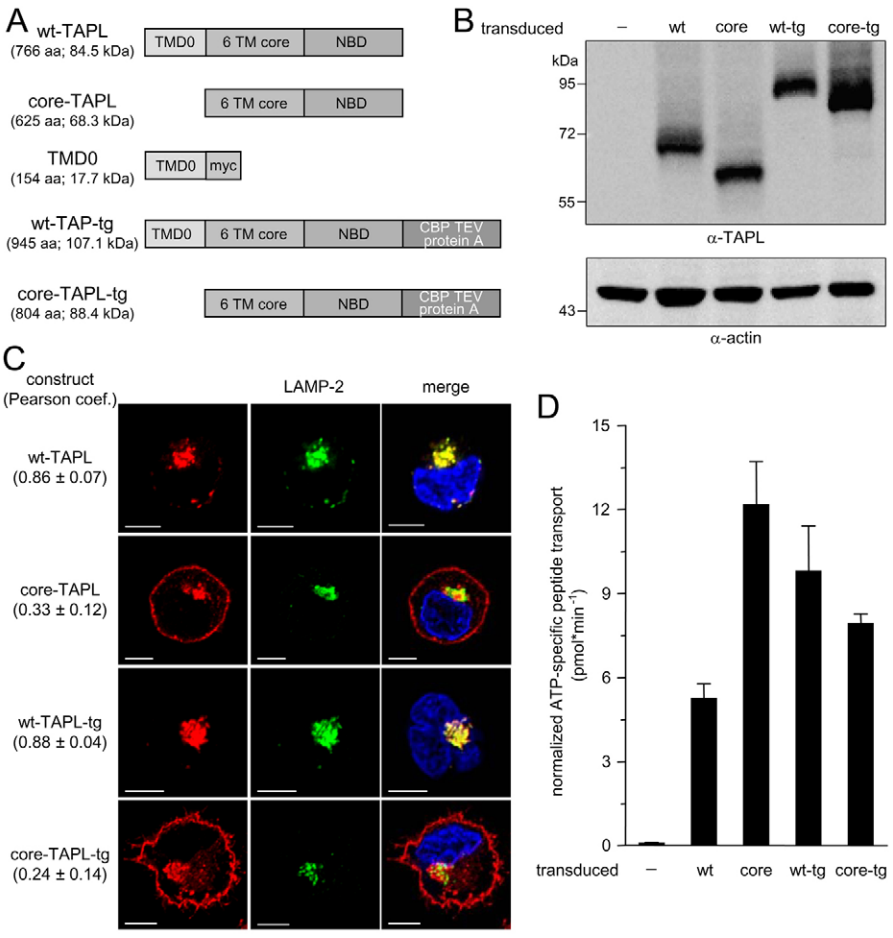

Fig. 1. Expression, localization and activity of TAPL variants in Raji cells. (**A**) Schematic representation of TAPL variants used in this study (CBP, calmodulin binding peptide; TEV, tobacco etch virus protease cleavage site; protein A, tandem protein A domain). (**B**) Expression of TAPL variants. Cells (2×10^5) transduced with wt, core or tandem affinity tagged (tg) TAPL and non-transduced cells were lysed in RIPA buffer and analyzed by SDS-PAGE followed by immunoblotting with anti-TAPL antibody. Equal loading was verified by actin staining. (**C**) Subcellular localization of TAPL variants. Raji cells expressing indicated constructs were stained with anti-TAPL antibody. Lysosomes were labeled with anti-LAMP-2 (2D5) antibody and the nucleus visualized with DAPI. For quantitative analysis, Pearson coefficients of 9–11 deconvoluted images are depicted in parentheses. Scale bars: 5 µm. (**D**) Transport activity. Crude membranes (100 µg protein) derived from non-transduced or cells transduced with indicated TAPL variants were incubated with fluorescein labeled peptide RRYC$^{(\Phi)}$KSTEL (2 µM) in the presence of ATP (3 mM) or AMP (3 mM) for 30 min at 32°C. Transported peptides were quantified by fluorescence ($\lambda_{ex/em}$=485/520 nm). ATP specific transport was calculated by subtracting background fluorescence in the presence of AMP. ATP dependent transport was normalized to the TAPL signal of the immunodetection. Since there was no western blot signal for TAPL in non-transduced Raji cells, these data were not normalized. The data represent the mean ± s.e.m. of triplicate measurements.

staining of core-TAPL seems to be associated with strong retrograde transport since core-TAPL is also detected in endolysosomal system which is even more pronounced in HeLa cells and mouse fibroblasts (supplementary material Fig. S2; Fig. 4A). Since the tandem affinity purification tag has a considerable size of 21 kDa, which could interfere with protein function, we analyzed transport activity of all TAPL variants. Remarkably, ATP-specific and TAPL-dependent accumulation of the fluorescein labeled peptide RRYC$^{(\Phi)}$KSTEL (Φ represents fluorescein coupled to a cysteine residue) in crude membranes was detected for all TAPL versions with small variations (Fig. 1D). Although Raji cells contain endogenous TAPL (Fig. 2F), Peptide transport could not be detected because of its low level. Since Raji cells express TAPL, this cell line is suitable to screen for interaction partners.

In conclusion, the tandem affinity purification tag fused to the C-terminus of full-length or core-TAPL does not interfere with expression, subcellular localization and biological function, which was an optimal starting point to use these constructs for the identification of interaction partners.

Identification of interaction partners of TAPL

For tandem affinity purification, single clones of stably transduced Raji cells with lowest expression of TAPL variants were isolated to minimize the risk of losing substoichiometrically expressed interaction partners. For isolation of full-length versions of TAPL, lysosomes were prepared by Percoll density gradient centrifugation (Demirel et al., 2007) whereas core-TAPL was purified from crude membranes because of its altered localization. For solubilization, the mild detergent digitonin was employed to preserve even weak interactions.

First, wt-TAPL with or without a tag was isolated by tandem affinity purification. Although both proteins were solubilized to the same extent, only wt-TAPL-tg was successfully purified showing the specificity of the isolation procedure (Fig. 2A). Besides TAPL, which migrates as an 80 kDa band in SDS-PAGE (10%), a protein of a molecular weight of 120 kDa co-eluted specifically with wt-TAPL-tg. To verify that the co-purified protein is a lysosomal interaction partner, we applied the same purification strategy to core-TAPL-tg. It could be also quantitatively isolated but no additional band at 120 kDa was detected (Fig. 2B).

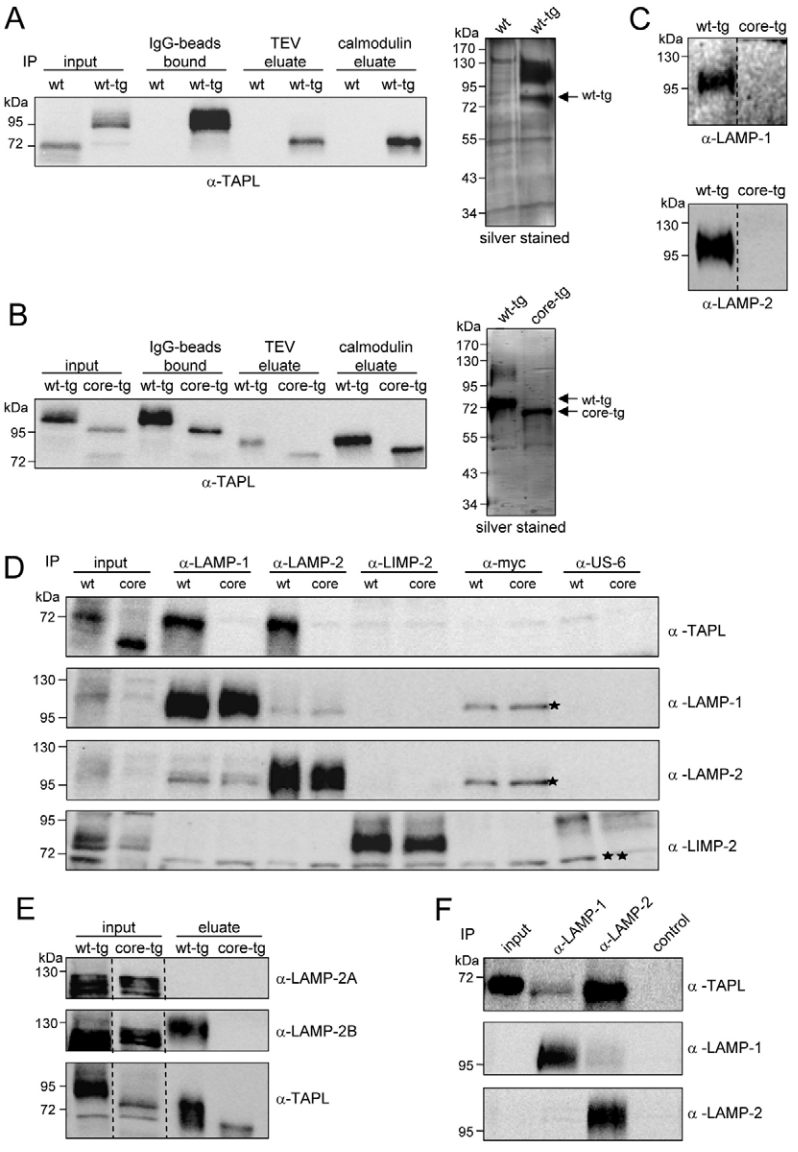

Fig. 2. Full-length TAPL interacts specifically with LAMP-1 and LAMP-2. For tandem affinity purification, membranes derived from Raji cells transduced with wt-TAPL, wt-TAPL-tg or core-TAPL-tg, respectively, were solubilized in 1% digitonin (input). After binding to IgG-agarose beads (IgG-beads bound), bound proteins were eluted by TEV-protease digestion (TEV eluate). In the second step, released proteins were purified by calmodulin-sepharose beads (calmodulin eluate). Purification of different constructs was compared by SDS-PAGE followed by silver staining and immunoblotting with anti-TAPL antibody. (**A**) Specificity of the tandem affinity purification. To depict the specificity of the tandem affinity purification, wt-TAPL or wt-TAPL-tg were purified site by site. (**B**) Lysosomal-specific interaction partners. To assign lysosome specific interaction partners, wt-TAPL-tg or core-TAPL-tg were simultaneously purified. (**C**) A fraction of the calmodulin eluate of wt-TAPL-tg and core-TAPL-tg was probed with anti-LAMP-1 (H4A3) and anti-LAMP-2 (2D5) antibodies. (**D**) Specific interaction with LAMP-1 and LAMP-2. Crude membranes (5 mg protein) from Raji cells containing wt or core-TAPL were solubilized with 1% digitonin. Immunoprecipitations were performed with indicated antibodies and analyzed on SDS-PAGE followed by immunoblotting with anti-TAPL antibody. Successful precipitations were verified by detection with antibodies against LAMP-1 (H4A3), LAMP-2 (2D5) or LIMP-2. Low intensities in input lanes are due to strong dilution of samples. (*, monoclonal antibodies used for immunoprecipitation and recognized by the secondary antibody of the immunodetection; **, cross-reactive band of the LIMP-2 antibody). (**E**) TAPL interacts specifically with LAMP-2B. A fraction of tandem affinity purified wt-TAPL-tg and core-TAPL-tg was separated by SDS-PAGE and analyzed with antibodies detecting specifically the LAMP-2 isoforms LAMP-2A or LAMP-2B. (**F**) TAPL expressed at endogenous levels. Crude membranes (10 mg protein) derived from non-transduced Raji cells were solubilized with 1% digitonin. Immunoprecipitations were performed with anti-LAMP-1 (H4A3) or anti-LAMP-2 (2D5) antibody, anti-myc was used as negative control. Eluates were analyzed on SDS-PAGE followed by immunoblotting with anti-TAPL antibody. Successful precipitations were verified by detection with antibodies against LAMP-1 and LAMP-2. Low input intensities are due to short exposure time to prevent overexposure of immunoprecipitated protein.

Table 1. Interaction partners of wt-TAPL determined by mass spectrometry[a]

Name	Accession No.	No. of different peptides	No. of total peptides	Sequence coverage
TAPL	Q9NP78	84	1120	47.0%
LAMP-1	P11279	9	28	16.6%
LAMP-2	P13473	6	54	11.7%
HLA-DR α-chain	P01903	4	26	16.5%
HLA-DRB1-1 β-chain	P04229	3	3	11.3%

[a]Proteins detected by more than two different peptides and localized to lysosomes are listed.

For determination of the interactome of TAPL, the purified samples were digested with trypsin and peptides were separated by two-dimensional liquid chromatography and sequenced by tandem mass spectrometry (2D-LC-tandem-MS). The pool of all proteins identified by more than two different peptides is depicted as supplementary material Table S1. To assign physiological interaction partners of wt-TAPL, the data were filtered considering only lysosomal proteins, which were identified by more than two different peptides (Table 1). wt-TAPL was detected with a sequence coverage of 47% and by 1120 peptides as the most frequent protein. As most abundant interaction partners, the lysosome-associated membrane proteins (LAMPs) LAMP-1 and LAMP-2 were found with a sequence coverage of 16.5% and 11.7%, respectively, which is high for these highly O- and N-glycosylated type I transmembrane proteins. The MHC class II subunits HLA-DR-α and -β were identified with lower frequency.

Taking the same selection filter for core-TAPL, which is not found in lysosomes, the list of possible interaction partners is larger than for wt-TAPL since it was purified from crude membranes instead of isolated lysosomes (Table 2 and supplementary material Table S2 for all proteins identified by more than two different peptides). Beside core-TAPL with a sequence coverage of 61%, different MHC class II subunits were co-purified (Table 2). Additionally, the small GTPase Rab-7a as well as nicastrin and presenilin-1 were found by this screen. Interestingly, all interaction partners of core-TAPL have a broad cellular distribution and are not restricted to the lysosomal compartment. Comparing the fingerprint analysis of tandem affinity purified full-length and core-TAPL, LAMP-1 and LAMP-2 seem to be specifically associated with full-length TAPL in lysosomes and represent the 120 kDa band as demonstrated by immunoblotting (Fig. 2C).

To verify these results by an orthogonal technique, crude membranes containing wt-TAPL or core-TAPL without any tag were solubilized by digitonin and proteins were immunoprecipitated by antibodies directed against the lysosomal membrane proteins LAMP-1, LAMP-2 and LIMP-2 (Fig. 2D). wt-TAPL was co-precipitated with LAMP-1 as well as with LAMP-2. However, wt-TAPL was not detected in the pull-down of LIMP-2 demonstrating the specific interaction with the LAMP proteins. Importantly, the core complex was not associated with any of these lysosomal membrane proteins as expected from its different subcellular localization.

For LAMP-2, three different splice variants are assigned with different cellular functions. The splice variants differ in exon 9, which codes for the 45 C-terminal residues comprising the transmembrane helix and the cytosolic tail of LAMP-2. By tandem affinity purification of core-TAPL-tg and wt-TAPL-tg derived from crude membranes of transduced Raji cells, we could demonstrate that wt-TAPL interacts with LAMP-2B but not with LAMP-2A, using splice variant specific antibodies for immunodetection (Fig. 2E). In accordance with previous results, core-TAPL did not show any interaction with one of these proteins. The association with the ill characterized LAMP-2C could not be analyzed since a specific antibody was not available.

Since all these studies were based on recombinant TAPL, we probed the interaction between these lysosomal membrane proteins by co-immunoprecipitation using non-transduced Raji cells, which express TAPL endogenously. Again, crude membranes were solubilized by digitonin and precipitated using LAMP-1 or LAMP-2 specific antibodies. Importantly, endogenous TAPL was co-precipitated with LAMP-1 as well as with LAMP-2 (Fig. 2F). In wt cells, significantly more TAPL was co-precipitated with LAMP-2 than with LAMP-1, whereas in stably transduced cells a similar amount of TAPL was isolated with either LAMP. These differences could be due to different affinities between TAPL and LAMP-1 and LAMP-2 or reflecting varying expression levels of LAMP proteins assuming none quantitative immunoprecipitation (Furuta et al., 1999). In conclusion, LAMP-1 and LAMP-2B are interaction partners of the lysosomal peptide transporter TAPL.

Probing the interaction of LAMP-1 and LAMP-2 with TAPL

To address the role of LAMP-1 and LAMP-2 in complex with TAPL, we stably transduced LAMP-1 and/or LAMP-2 deficient mouse embryonic fibroblasts with human wt-TAPL or core-TAPL, since there are no LAMP-1/2 deficient human cell lines available. Both TAPL variants were expressed in LAMP positive

Table 2. Interaction partners of core-TAPL determined by mass spectrometry[a]

Name	Accession No.	No. of different peptides	No. of total peptides	Sequence coverage
TAPL	Q9NP78	143	983	61.0%
Ras-related protein Rab-7a	P51149	10	20	31.4%
HLA-DQ(1) β-chain	P01918	8	8	23.0%
HLA-DR α-chain	P01903	11	78	21.3%
HLA-DRB1-1 β-chain	P04229	10	55	19.2%
Nicastrin	Q92542	6	8	11.8%
HLA-DRB1-10 β-chain	Q30167	4	5	11.3%
Presenilin-1	P49768	3	3	10.1%

[a]Proteins detected by more than two different peptides and localized to lysosomes are listed.

as well as in LAMP-1, LAMP-2 or LAMP-1/2 deficient cell lines (Fig. 3A). Lower expression of TAPL in LAMP-1 or LAMP-1/2 deficient MEFs seems to result from differences in number and location of genetic integrations. Importantly, no aggregates of TAPL were detected in the immunoblot (supplementary material Fig. S3). Therefore, the LAMP proteins seem not to be important for correct folding of the peptide transport complex. Moreover human TAPL, which shows 93% sequence identity with mouse TAPL, associates with mouse LAMP-1 and LAMP-2, as probed by co-immunoprecipitation. Nevertheless, neither LAMP-1 nor LAMP-2 were co-precipitated with core-TAPL implicating that mouse LAMP molecules interact in the same manner as the human counterparts with TAPL (Fig. 3B). Therefore, the mouse cell lines can be used to dissect the interaction between LAMP and human TAPL. Strikingly, in single deficient cell lines, wt-TAPL is still associated with the remaining LAMP (Fig. 3B). In conclusion, the interaction of LAMP-1 and LAMP-2 with the TAPL complex is independent from each other.

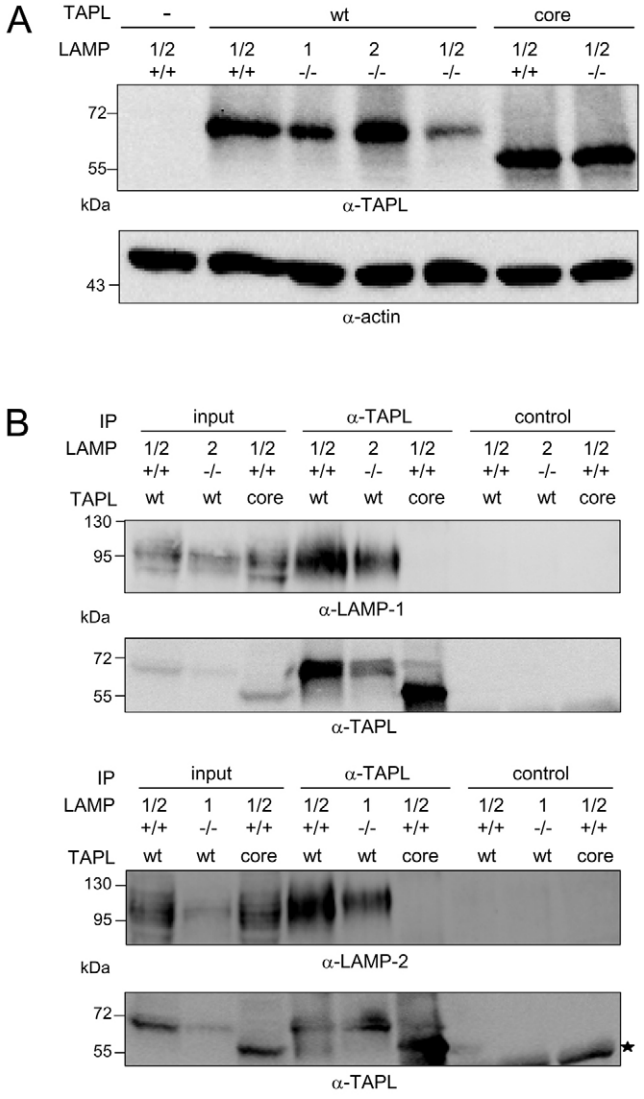

Fig. 3. TAPL interacts independently with LAMP-1 and LAMP-2. (**A**) Expression of TAPL variants in MEFs. MEF-wt (+/+), LAMP-1-deficient (1-/-), LAMP-2-deficient (2-/-) as well as LAMP-1 and LAMP-2 double deficient (1/2-/-) cells were transduced with indicated constructs. Non-transduced or transduced cells were lysed in RIPA buffer and 1×10^5 cells were separated by SDS-PAGE. After immunoblotting, TAPL was detected with anti-TAPL antibody. Equal loading was verified by actin staining. (**B**) TAPL interacts with murine LAMP-1 and LAMP-2. Cells from wild-type or LAMP-1 or LAMP-2 single-deficient MEF cells transduced with indicated constructs were solubilized in 1.5% digitonin. Co-immunoprecipitations were performed with anti-TAPL antibody or anti-MDL1 antibody as control. Eluates were separated on SDS-PAGE followed by immunoblotting with anti-LAMP-1 (1D4B), anti-LAMP-2 (ABL93) and anti-TAPL antibodies (*, polyclonal antibody used for immunoprecipitation and recognized by the secondary antibody of the immunodetection).

To exclude artificial interactions between TAPL and LAMP-1 and LAMP-2 during cell lysis, we mixed digitonin solubilized lysates of wt MEFs (non-transduced) and TAPL transduced LAMP-1/2 deficient MEFs. Under these conditions, neither LAMP-1 nor LAMP-2 was co-precipitated with TAPL (supplementary material Fig. S4A). Moreover, solubilization of TAPL transduced wt MEFs at neutral pH or pH 5, typically found in lysosomes, had no impact on the interaction (supplementary material Fig. S4B). Therefore, the interaction between TAPL and LAMP-1 and LAMP-2 is formed in the cell and is not influenced by the neutral pH of the solubilization conditions.

Functional interaction of LAMP and TAPL

To identify the relevance of the interaction of LAMP-1 and LAMP-2 with TAPL, we characterized the function of TAPL in different MEF cells in detail. Lysosomal targeting often relies on special double leucine based or tyrosine containing sequences in the cytosolic, membrane proximal part of membrane proteins (Bonifacino and Traub, 2003). Since TAPL does not possess such a sequence, we examined whether the LAMP proteins escort this peptide transport complex into lysosomes as shown for MHC class II complexes escorted by the invariant chain (Lotteau et al., 1990). Therefore, immunofluorescence microscopy of MEFs stably transduced with wt- or core-TAPL was applied to determine subcellular localization. Independent of LAMP-1 or LAMP-2, wt-TAPL trafficked to lysosomes as demonstrated by the co-localization with the lysosomal marker protein LIMP-2 as reflected by a Pearson correlation coefficient of 0.50 to 0.66 (Fig. 4A). As in human cells, core-TAPL showed a more diffuse distribution with only a minor portion overlapping with the lysosomal marker. Since the localization of wt-TAPL in LAMP positive or deficient cell lines is the same, neither LAMP-1 nor LAMP-2 is involved in the subcellular targeting of TAPL.

To investigate the transport activity of TAPL in dependence on LAMP-1 and LAMP-2, peptide translocation was studied in saponin semi-permeabilized cells. Independent of the presence or absence of the LAMP proteins, similar ATP-specific and TAPL-dependent transport was detected for wt, single and double LAMP deficient cell lines whereas in non-transduced MEFs no peptide translocation could be detected (Fig. 4B). Thus, the interaction of TAPL with LAMP-1 and LAMP-2 has no impact on TAPL activity.

Protein interactions often have a stabilizing effect on proteins in respect of inactivation or degradation. To test the influence of LAMP-1/2 on thermal inactivation of TAPL, we incubated membranes derived from wt and LAMP-1/2 deficient MEFs for increasing time at 37℃ and analyzed subsequently peptide transport activity. TAPL activity diminished in the presence and

absence of LAMP proteins with similar rates indicating that the LAMP proteins do not protect TAPL against thermal denaturation (Fig. 4C).

To investigate further the stability of TAPL, we studied the half-life of TAPL in dependence on the LAMP proteins. Therefore, mouse embryonic fibroblasts transduced with

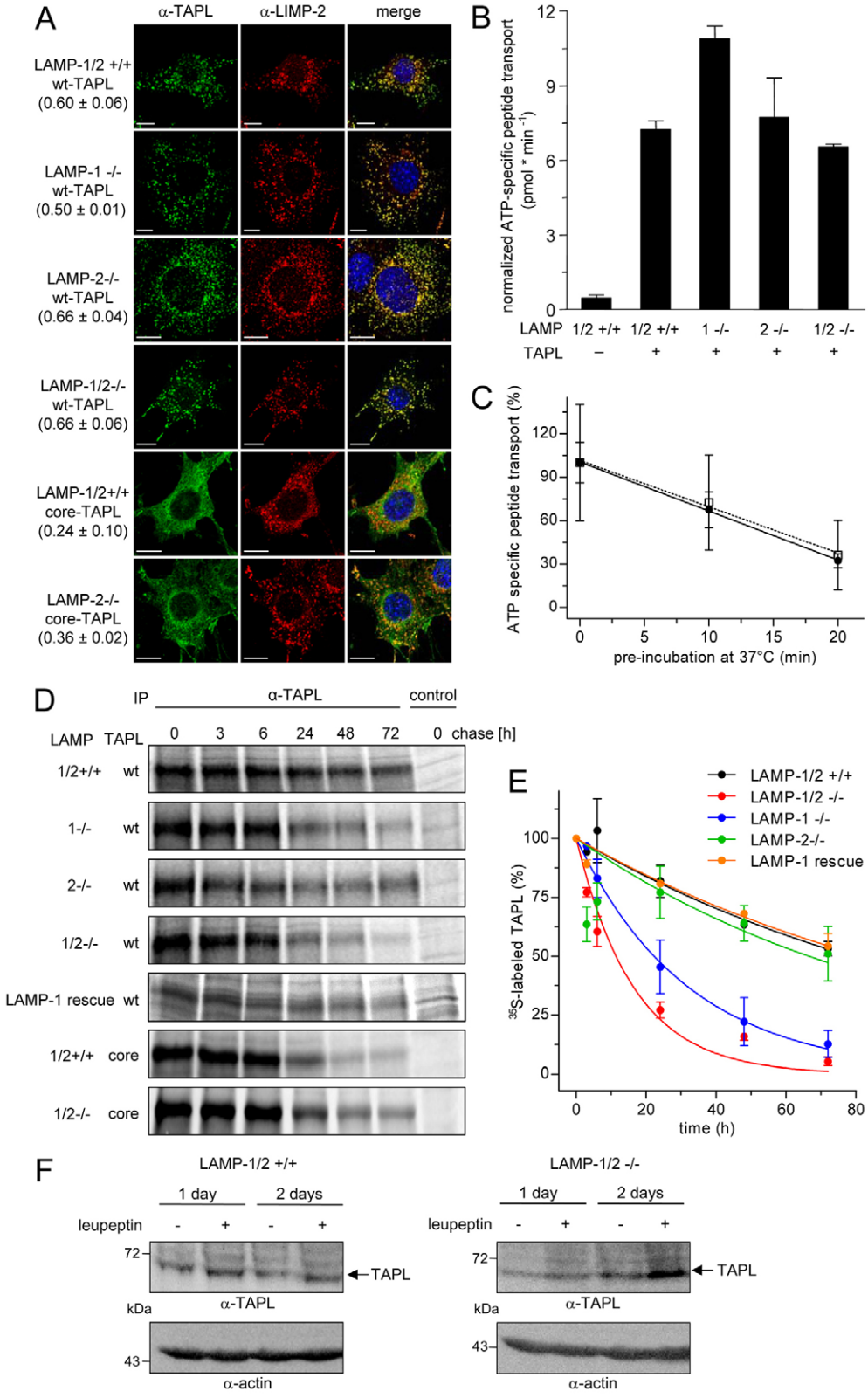

Fig. 4. See next page for legend.

wt-TAPL or core-TAPL were pulsed with [^{35}S]-labeled cysteine and methione for three hours and chased for the indicated time points. Subsequently, TAPL was isolated by immunoprecipitation and visualized by autoradiography (Fig. 4D). Independent of the presence of LAMP-1 and LAMP-2, strong signals of TAPL were detected immediately after the pulse time indicating that TAPL translation is not influenced by LAMP-1 or LAMP-2. In wt-cells the TAPL signal decreased slowly with a half-life of 79 h. In cells deficient of LAMP-1 or LAMP-2 half-life of TAPL decreased to 22 h and 66 h, respectively, showing different effects of LAMP variants. Both LAMP proteins seem to have a synergistic effect, since in LAMP-1/2 deficient cells TAPL signal disappeared fastest with a half-life of 11 h. Importantly, by co-transduction of LAMP-1/2 deficient MEFs with TAPL and murine LAMP-1, half-life of TAPL was restored to 82 h demonstrating the direct influence of LAMP on the stability of TAPL independent from genetic variations of different MEFs. Core-TAPL, which does not interact with either LAMP-1 or LAMP-2, showed independently of LAMP a half-life of 15 h, comparable with wt-TAPL in the absence of LAMP-1 and LAMP-2 (Table 3; supplementary material Fig. S5). Notably, LAMP-1 or LAMP-2 does not influence the overall stability of lysosomal proteins as demonstrated by similar stability of LIMP-2 in wt as well as in LAMP-1 and LAMP-2 double deficient cell lines (supplementary material Fig. S5) and as reported for soluble as well as membrane bound lysosomal proteins as cathepsin D, NPC2 and NPC1 (Eskelinen et al., 2004).

To test whether reduced half-life of TAPL in the absence of LAMP-1/2 depends on faster proteolytic degradation, we compared the steady state level of TAPL in wt MEFs and LAMP-1/2 deficient MEFs in the presence and absence of the lysosomal protease inhibitor leupeptin (Aniento et al., 1993). In wt MEFs, the steady state level of TAPL did not change during two days of leupeptin treatment confirming the long half-life of TAPL by the stabilizing effect of the LAMP proteins. However, in LAMP-1/2 knockout cells, the level of TAPL increased in leupeptin treated cells demonstrating that the LAMP proteins protect TAPL from lysosomal degradation (Fig. 4F). In conclusion, LAMP-1 strongly stabilizes TAPL by protection from lysosomal degradation, whereas LAMP-2 has a minor impact.

Fig. 4. Impact of LAMP interaction on TAPL function. (**A**) Subcellular localization of TAPL. In MEF cells with indicated LAMP deficiencies, stably transduced wt- or core-TAPL was detected with anti-TAPL antibody conjugated to Dylight 488. Lysosomes were visualized by rabbit-LIMP-2 antibody followed by anti-rabbit-Cy3 staining. For quantitative analysis, Pearson coefficients of 9–11 deconvoluted images are depicted in parentheses. Scale bars: 10 μm. (**B**) Activity of TAPL. Different MEFs (2.5×10^6 cells) were semi-permeabilized with saponin and incubated with fluorescein-labeled peptide RRYC$^{(\Phi)}$KSTEL (5 μM) in the presence of ATP (10 mM) or AMP (10 mM) for 3 min at 32℃. Transported peptides were quantified by fluorescence ($\lambda_{ex/em}$=485/520 nm). ATP-specific transport was calculated by subtracting background fluorescence in the presence of AMP. ATP-dependent transport was normalized to the TAPL signal of the immunodetection. Since there was no Western blot signal for TAPL in non-transduced MEFs, these data were not normalized. The data represent the mean ± s.e.m. of triplicate measurements. (**C**) Thermal stability of TAPL in MEF cell variants. Crude membranes (100 μg protein) derived from stably TAPL-transduced MEF wt (filled dots, filled line) or cells deficient in LAMP-1 and LAMP-2 (open square, dotted line) were incubated for 0, 10 or 20 min at 37℃. Subsequently, transport was performed with peptide RRYC$^{(\Phi)}$KSTEL (2 μM) in the presence of ATP (3 mM) or AMP (3 mM) for 30 min at 32℃ and ATP-specific transport was determined. Data were fitted by linear regression, resulting in destabilization rate of -3.4 ± 0.1 min^{-1} and -3.2 ± 0.3 min^{-1} for wt and LAMP-1- and LAMP-2-deficient cells, respectively. The data represent the mean ± s.e.m. of triplicate measurements. (**D**) Pulse-chase labeling. Different MEFs stably expressing wt-TAPL or core-TAPL were metabolically labeled with [^{35}S]Cys/Met for 3 h and chased for the indicated time points. In a restoration experiment, LAMP-1/2-deficient MEFs co-transduced with wt-TAPL and murine LAMP-1 (LAMP-1 rescue) were pulsed identically. Harvested cells were solubilized in RIPA buffer and immunoprecipitations were performed with anti-TAPL antibody or anti-US-6 antibody as control. Eluates were loaded on SDS-PAGE, electroblotted on nitrocellulose and precipitation products were detected with a Typhoon phosphorimager. (**E**) Quantification of pulse-chase labeling. Signals were quantified and time points were fitted by monoexponential decay. Data are represented as mean ± s.e.m. from two to three independent experiments. Half-lives are given in Table 3. (**F**) Proteolytic protection of TAPL. Stable TAPL-transduced MEF wt or cells deficient in LAMP-1 and LAMP-2 were incubated for up to 2 days with or without 10 μM leupeptin. Cells (5×10^5) were lysed in RIPA buffer and analyzed by SDS-PAGE followed by immunoblotting with anti-TAPL antibody. Equal loading was verified by actin staining.

Identification of the interaction domain in TAPL

Although a minor portion of core-TAPL was found in lysosomes, we never observed any interaction with LAMP-1 or LAMP-2 (Fig. 2C, Fig. 3B) indicating that the unique N-terminal TMD0 of TAPL, which redirects core-TAPL by non-covalent interactions into lysosomes (Demirel et al., 2010), could represent the interaction domain. To prove this hypothesis, we stably expressed TMD0 (residues 1-142) containing a C-terminal myc-tag in wild type, LAMP-1 and/or LAMP-2 deficient mouse embryonic fibroblasts by retroviral transduction (Fig. 1A; supplementary material Fig. S7). In all cell lines, TMD0 was found in the lysosomal compartment (supplementary material Fig. S6). To probe the interaction, wt MEFs were lysed by digitonin and LAMP-1 or LAMP-2 was immunoprecipitated (Fig. 5A). Under both conditions, TMD0 was co-precipitated. Additionally, in single deficient cell lines TMD0 was co-purified with the remaining LAMP, showing that this unique domain independently interacts with each of the LAMP proteins.

To investigate that TMD0 mediates the interaction between core-TAPL and LAMP-1 or LAMP-2, MEFs were co-transduced with TMD0 and core-TAPL. By immunoprecipitation of LAMP-1 or LAMP-2, TMD0 as well as core-TAPL were simultaneously co-precipitated, demonstrating that TMD0 restores the interaction between the core complex and LAMP-1 and LAMP-2 (Fig. 5B) since core-TAPL expressed alone was never in complex with LAMP proteins (Fig. 2C,D, Fig. 3B). Taken together, TMD0 mediates the interaction between core-TAPL and the LAMP proteins.

Discussion

In the present study, we have identified a new role for the lysosomal membrane proteins LAMP-1 and LAMP-2B as interaction partners of the peptide transport complex TAPL. Notably, LAMP-2A, the receptor of chaperone mediated autophagy, does not interact with TAPL. The binding site of LAMP proteins is restricted to the unique N-terminal TMD0 of TAPL. The complex formation is neither required for lysosomal targeting of the peptide transporter nor for its transport activity but strongly increases TAPL stability by decreasing proteolytic degradation.

Table 3. LAMP-dependent stability of TAPL

MEF	TAPL variant	half-life (h)
wt	wt	79
LAMP-1$^{-/-}$	wt	22
LAMP-2$^{-/-}$	wt	66
LAMP-1/2$^{-/-}$	wt	11
LAMP-1/2$^{-/-}$ rescued with mLAMP-1	wt	82
wt	core	15
LAMP-1/2$^{-/-}$	core	15

By tandem affinity purification and co-immunoprecipitation, LAMP-1 and LAMP-2B were identified as binding partners of TAPL. Importantly, these interactions could be verified also in non-transduced cells, showing that these are not artificial contacts due to high expression of recombinant proteins. Moreover, TAPL binds specifically to LAMP-1 and LAMP-2B but not to the splice variant LAMP-2A and also not to the abundant lysosomal membrane protein LIMP-2. We also excluded that TAPL and LAMPs associate after solubilization by mixing cell lysate of TAPL transduced MEFs deficient of LAMP-1 and LAMP-2 with a lysate of wt MEFs.

Interestingly, MHC class II subunits were identified as an additional interaction partner of TAPL. This complex seems to appear with low frequency since MHC class II subunits could not be found by immunodetection of tandem affinity purified or immunoprecipitated TAPL and the amount of peptides sequenced by tandem mass spectrometry was much lower than for LAMP-1 and LAMP-2B. The low abundance of this complex could result from a very transient interaction, and therefore mostly lost during isolation, or it could imply that only a subset of TAPL molecules is associated with MHC class II molecules. MHC class II molecules were also detected by tandem affinity purification of core-TAPL implying that the core complex is sufficient for this interaction, which is not restricted to the lysosomal compartment. Strikingly, TAPL and intracellular MHC class II expression overlaps (Demirel et al., 2010) and the expression of TAPL is strongly upregulated in professional antigen presenting cells (Demirel et al., 2007). Therefore, it can be speculated that in professional antigen presenting cells the interaction with MHC class II molecules has a functional impact on loading of antigenic peptides derived from cytosol by TAPL increasing the diversity of antigenic peptides.

The interaction of LAMP-1 and LAMP-2B with TAPL differentially increases the half-life of TAPL by protecting TAPL from proteolytic degradation. However, these interactions have neither an impact on the subcellular targeting of TAPL nor on the transport function or thermostability of TAPL. The half-lives of LAMP-1 (ca. 50 h) (Isaac et al., 2000) and LAMP-2 (ca. 70 h) (Andrejewski et al., 1999) are comparable with that of TAPL. Strikingly, LAMP-1 displays a stronger stabilization effect than LAMP-2 although LAMP-2 deficiency has a much more unfavourable effect on mice, showing accumulation of autophagic vacuoles, malfunction in lysosomal protein targeting and defects in cholesterol homeostasis (Eskelinen et al., 2002; Eskelinen et al., 2004; Tanaka et al., 2000). Moreover, LAMP-1 deficiency seems to be compensated by increased LAMP-2 expression (Andrejewski et al., 1999). Therefore, the stabilization of TAPL seems to be a direct effect of the specific interaction and not due to a more general effect on lysosome stability and biogenesis supported by the unaffected half-life of LIMP-2 and other soluble and membrane proteins of lysosomes (Furuta et al., 1999). The half-life of core-TAPL, which does not interact with LAMP and which is predominantly trafficked to the plasma membrane, is comparable with wt-TAPL in the absence of the LAMP proteins.

Post-Golgi integral membrane proteins destined for degradation are typically directed into the limiting membrane of endosomes by a mono-ubiquitin dependent or independent mechanism (Reggiori and Pelham, 2001). Subsequently, membrane proteins are incorporated into intraluminal vesicles (ILVs) by budding from the limiting membrane of late

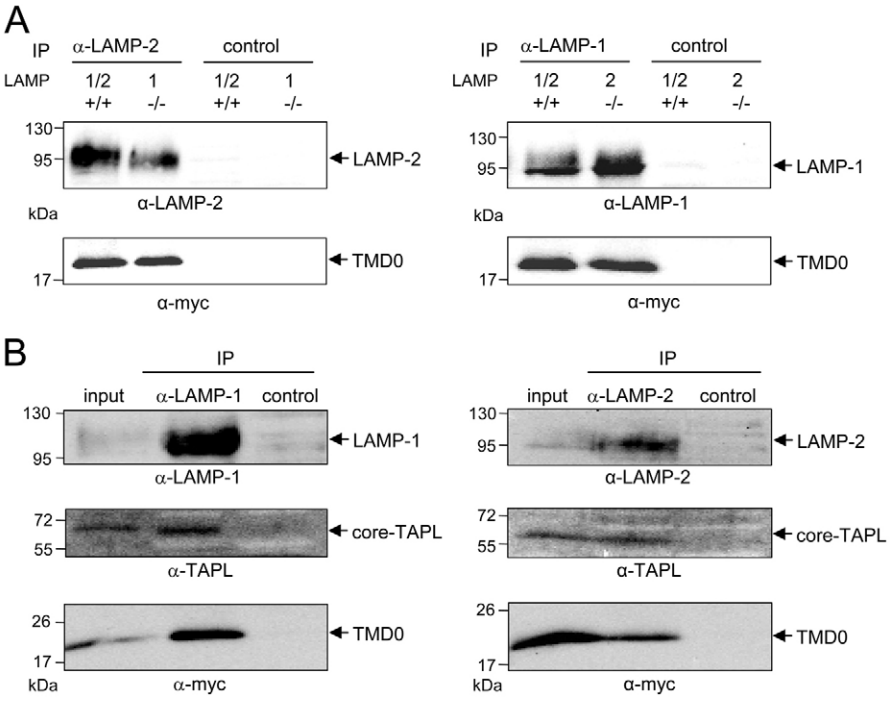

Fig. 5. Identification of the interaction domain within TAPL. (**A**) TMD0 physically interacts with LAMP-1 and LAMP-2 in MEF wt and single-deficient cells. MEFs (2×10^7 cells) stably expressing TMD0 were solubilized with 2% digitonin and TMD0 was co-immunoprecipitated with anti-LAMP-2 (ABL93), anti-LAMP-1 (1D4B) or anti-tapasin (7F6) antibody as control. The eluates were separated by SDS-PAGE (5–15%) followed by immunoblotting using indicated antibodies. (**B**) TMD0 mediates the interaction between core-TAPL and the LAMP proteins. MEFs (2×10^7 cells) stably co-expressing TMD0 and core-TAPL were solubilized by digitonin and immunoprecipitation was performed with anti-LAMP-1 (1D4B), anti-LAMP-2 (ABL93) or anti-tapasin (7F6) antibody as control. Samples were separated by SDS-PAGE (5–15%) followed by immunoblotting using indicated antibodies.

endosomes, forming multivesicular bodies which fuse with lysosomes to release ILVs into the lysosomal lumen for degradation (Piper and Katzmann, 2007). LAMP-1 and LAMP-2 are found predominantly in lysosomes and the limiting membrane of MVBs and are hardly detected on intraluminal vesicles (Escola et al., 1998). Therefore, it can be speculated that the interaction with LAMPs retains TAPL from incorporation into the intraluminal vesicles and therefore stabilizes the polypeptide transport complex against lysosomal degradation.

Notably, the LAMP proteins interact independently with TAPL and both proteins show a stabilizing effect as demonstrated with the single deficient cell lines. However, the stoichiometry of this peptide transport complex is not solved yet. LAMP-2B but not LAMP-2A binds to TAPL. These splice variants differ in exon 9, including the transmembrane helix and the cytosolic 11 residues comprising the C-terminal tail. The strongest difference between these alternative splice variants resides in the cytosolic tail. Additionally, the C-terminal tail of LAMP-1 shows a higher similarity to LAMP-2B than to LAMP-2A. The cytosolic tail of LAMP-2A displays the docking site for the cytosolic chaperone machinery delivering substrate for chaperone mediate autophagy (Cuervo and Dice, 2000). It will be interesting to see whether the cytosolic tails of LAMP-1 and LAMP-2B are indeed involved in the interaction with TAPL.

The unique N-terminal TMD0 of TAPL forms the interaction site with LAMP-1 and LAMP-2. The endoplasmic reticulum localized antigen transporter TAP, showing a sequence homology of ca. 40% with TAPL, binds via its TMD0 to the type I glycoprotein tapasin (Koch et al., 2004) which stabilizes this peptide transporter (Lehner et al., 1998). Moreover, the TMD0 of the sulfonylurea receptor 1 mediates the interaction with the potassium channel Kir6.2 and influences its trafficking and gating (Chan et al., 2003).

Altogether, TMD0 of TAPL takes over a dual function. It targets the core complex into lysosomes and it displays the interaction platform with the LAMP proteins. Future studies will be necessary to identify this interaction on molecular level.

Materials and Methods

Materials

Peptides were synthesized by Fmoc [N-(9-fluorenyl)methoxycarbonyl] solid phase chemistry and labeled by iodoacetamidofluorescein (Neumann and Tampé, 1999). For immunofluorescence microscopy, immunodetection, and immunoprecipitation the following antibodies were used: rabbit anti-TAPL (Wolters et al., 2005), rabbit anti-Mdl1 (Gompf et al., 2007), rabbit anti-US-6 (Kyritsis et al., 2001), mouse anti-myc (Millipore, Schwalbach, Ts., Germany), rat anti-human-tapasin (7F6) (Koch et al., 2004), rabbit anti-human-LAMP-2A, rabbit anti-human-LAMP-2B (Abcam, Cambridge, UK), mouse anti-human-LAMP-2 (2D5) (Radons et al., 1992), mouse anti-human-LAMP-1 (H4A3), rat anti-mouse-LAMP-1 (1D4B), rat anti-mouse-LAMP-2 (ABL93) (Developmental Studies Hybridoma Bank, Iowa, USA), rabbit anti-human/mouse-LIMP-2 (Abcam) or rabbit anti-mouse-LIMP-2 (Reczek et al., 2007); mouse anti-cation independent (ci) mannose-6-phosphate receptor (Abcam), mouse anti-58K, Golgi protein (Abcam), mouse anti-MHC class I (W6/32) (Abcam), fluorophor-labeled antibodies Cy3 goat anti-rabbit IgG (Dianova, Hamburg, Germany), Cy3 donkey anti-mouse IgG (Dianova), Alexa488 goat anti-rat (Invitrogen, Karlsruhe, Germany) or Alexa488 donkey anti-mouse (Invitrogen) and horseradish peroxidase conjugated secondary antibodies goat anti-rabbit (BD Pharmingen, Heidelberg, Germany) and goat anti-mouse (Sigma-Aldrich, Munich, Germany).

Cell lines and culture

293T and mouse embryonic fibroblasts (MEFs) (wt, LAMP-1, LAMP-2 or LAMP-1/LAMP-2 double deficient) were cultured in DMEM (PAA Laboratories, Coelbe, Germany) with 10% fetal calf serum (Biochrom AG, Berlin, Germany), 2 mM L-glutamine, 100 µg/ml penicillin and 100 µg/ml streptomycin. To test the proteolytic degradation of TAPL, 10 µM of leupeptin (Applichem, Darmstadt, Germany) was added to the medium and leupeptin was replaced every 24 h. Human Burkitt lymphoma cells (Raji cells) were grown in RPMI 1640 (PAA Laboratories) with 10% fetal calf serum (Biochrom AG), 1 mM sodium pyruvate, 10 mM HEPES, 2 mM L-glutamine, 100 µg/ml penicillin and 100 µg/ml streptomycin. For Raji cells stably transduced with pLPCX or pZome-1-C constructs, medium was supplemented with 0.5 µg/ml puromycin (Sigma-Aldrich).

Cloning

Cloning of human wt-TAPL, core-TAPL (aa 143-766 containing an N-terminal methionine) and TMD0 (aa 1-142 containing a C-terminal myc-tag) into pLPCX and pMSCV-IRES-Thy1.1 vectors were described previously (Demirel et al., 2010). wt-TAPL or core-TAPL was cloned into pZome-1-C (Euroscarf, University of Frankfurt a.M., Germany) resulting in constructs with a C-terminal tandem affinity purification tag consisting of calmodulin binding peptide and protein A separated by a TEV cleavage site. Following forward primers were used for PCR amplification 5′-CGGGATCCCGGCCACCATGCGGCTGTGGAAGG-3′ (TAPL-wt) or 5′-CG-ATTAGGATCCATGGGCACCCAGGCCCTGGAG-3′ (core-TAPL). The same reverse primer 5′-CGATTAGGATCCGGCCTTGTGACTGCC-3′ was used for both. BamHI digested PCR products were ligated into pZome-1-C. The murine LAMP-1 gene was PCR-amplified using the following primers: 5′-CGATTAAT-CGATCTAGATGGTCTGATAGCCGGCG-3′ and 5′- CGATTAGAATTCATGG-CGGCCCCCGG-3′. The PCR product was cloned via ClaI and EcoRI restriction sites into the retroviral pLPCX vector (Clontech, Saint-Germain-en-Laye, France).

Retroviral transduction

Production of recombinant retroviruses were described previously (Demirel et al., 2007). For transduction of Raji cells, pLPCX based viral particles were used and positive cells were selected with puromycin. Raji cells expressing untagged wt-TAPL or core-TAPL are bulk cultures. For tandem affinity purification, single clones expressing lowest levels of TAPL-tg or core-TAPL-tg were selected. MEF cells were transduced with retrovirus generated with pMSCV-IRES-Thy1.1 constructs and sorted via magnetic beads using CELLection Biotin Binder Kit (Invitrogen) following manufacturer's instructions. To generate MEF cells co-expressing TMD0 and core-TAPL, sorted TMD0-expressing cells were transduced with core-TAPL (pLPCX) and subsequently selected by puromycin. For double transduction with murine LAMP-1 and human TAPL, MEFs deficient in LAMP-1 and -2 were transduced with murine LAMP-1 (pLPCX) and human TAPL (pMSCV-IRES-Thy1.1) simultaneously. Cells were subsequently sorted via magnetic beads and grown in the presence of puromycin.

Preparation of crude membrane

Cells were thawed on ice and resuspended in Tris buffer (20 mM Tris-HCl, 1 mM DTT, 2.5 mM benzamidine hydrochloride, 1 mM PMSF, pH 7.4). The cells were lysed with 40 strokes in a tight fitting Dounce homogenizer. Subsequently, sucrose was added to a final concentration of 250 mM. Nuclei and cell debris were pelleted by centrifugation at 200 ***g*** for 4 min followed by 8 min at 700 ***g***. Crude membranes were harvested by centrifugation at 20,000 ***g*** for 25 min at 4℃. Membranes were resuspended in ice cold PBS, snap-frozen in liquid nitrogen and stored at −80℃.

Preparation of lysosomes

For tandem affinity purification, 1×10^9 cells were harvested by centrifugation for 5 min at 300 ***g*** and washed in homogenization buffer (10 mM HEPES, 1 mM EDTA, 250 mM sucrose, 2.5 mM benzamidine hydrochloride, 1 mM PMSF, pH 7.4). Cells were resuspended in homogenization buffer and lysed with a tight fitting Dounce homogenizer until 90% of cells were disrupted. The homogenate was centrifuged twice at 1000 ***g*** for 5 min and the post-nuclear supernatant was layered on 31% (v/v) Percoll which was underlaid with a cushion of 27.6% Nycodenz solution. The gradient was centrifuged in a swing-out rotor at 40,000 ***g*** for 1 h. The fraction with the highest Percoll concentration contained lysosomes.

Tandem affinity purification

Purifications were performed either with isolated lysosomes for wt-TAPL and TAPL-tg or with crude membranes for core-TAPL (Demirel et al., 2007). Lysosomes or membranes were solubilized in buffer containing 20 mM Tris-HCl (pH 7.4), 150 mM NaCl, 1% digitonin (Roth, Karlsruhe, Germany), 15% glycerol, 2 mM EDTA and 1% protease inhibitor mix (Serva, Heidelberg, Germany) for 1 h on ice and centrifuged at 100,000 ***g*** for 45 min. Cleared lysates were incubated with 400 µl of human IgG-agarose beads (Sigma-Aldrich) for 2–4 h at 4℃. Beads were washed first with 20 mM Tris-HCl (pH 7.4), 150 mM NaCl, 0.1% digitonin and 15% glycerol and then with TEV-protease cleavage buffer (10 mM Tris-HCl, pH 8.0, 150 mM NaCl, 0.1% digitonin, 15% glycerol, 0.5 mM EDTA and 1 mM DTT). Bound proteins were eluted by addition of 100 units AcTEV protease (Invitrogen) overnight at 4℃. The cleavage product was incubated with 400 µl calmodulin Sepharose beads (GE Healthcare, Munich, Germany) in the presence of 6 mM $CaCl_2$. After washing with calmodulin binding buffer (10 mM Tris-HCl, pH 7.4, 150 mM NaCl, 0.1% digitonin, 15% glycerol, 2 mM $CaCl_2$ and 10 mM mercaptoethanol), final elution was performed with calmodulin binding buffer containing 25 mM EGTA instead of $CaCl_2$. For

SDS-PAGE and immunoblotting, final eluate was concentrated with Strataclean beads (Stratagene, Waldbronn, Germany). For mass spectrometry analysis, eluted proteins were precipitated with acetone overnight at −20℃.

Mass spectrometry

Prior to mass spectrometric detection, proteins were treated with trypsin and peptides were separated using a MudPIT system according to Washburn et al. (Washburn et al., 2001) consisting of a custom-made biphasic column within a fused-silica ESI emitter tip coupled online to an LTQ XL mass spectrometer (Thermo Fisher Scientific, San Jose, CA). The biphasic separation column consisted of a 13 cm Luna C18 separation phase (Luna C18 RP, 3 µm, Phenomenex, Aschaffenburg, Germany), which has been directly packed into the nanotip followed by a 5 cm SCX phase (PolySULFOETHYL^{TM}, 3 µm, Chromatographic Technologies, Basel, Switzerland). For sample pre-concentration, a 3 cm Luna C18 phase was used on top as trapping phase. Flow rate for all applications was 250 nl/min. For a 9 step MudPIT experiment, each step was represented by one instrument method file with identical settings except for the gradient program for the HPLC. The four buffer solutions used for the chromatography were 2% acetonitrile/0.1% formic acid (buffer A), 80% acetonitrile/0.1% formic acid (buffer B), 250 mM ammonium acetate (buffer C), and 1.5 M ammonium acetate (buffer D). The first step of 180 min duration consisted of a 160 min gradient from 0 to 100% buffer B, a 10 min hold at 100% buffer B, and a 10 min re-equilibration step with buffer A. The next 7 steps were 130 min long each with the following profile: 5 min of 100% buffer A, 2 min of x% buffer C, 3 min of 100% buffer A, a 10 min gradient from 0 to 7% buffer B and a 90 min gradient from 7 to 35% buffer B followed by a 10 min hold at 100% buffer B and a 10 min re-equilibration step with buffer A. The 2 min buffer C percentages (x) in steps 2–8 were as follows: 10, 20, 30, 40, 50, 70, and 100%. Step 9 consisted of the following profile: A 5 min buffer A wash was followed by a 20 min 100% buffer D wash, a 5 min 100% buffer A wash, a 10 min gradient from 0 to 10% buffer B, and a 90 min gradient from 10 to 45% buffer B. Step 10 was finalized by a 10 min hold at 100% buffer B and a 10 min re-equilibration step with buffer A. Mass spectrometric detection was performed by acquiring one full MS scan with a scan range from 400 to 2000 followed by MS/MS spectra of the three most intensive ions with normalized collision energy of 35%. Dynamic exclusion was set to 30 s with a range of ±1.5 Da.

To interpret MS/MS, data we used the SEQUEST algorithm, implemented in Bioworks 3.3.1. Data were searched against all human entries in the Swiss-Prot (v.55) database. All accepted results had a ΔCn value of 0.08 or higher. Singly, doubly, and triply charged peptides had to be partially tryptic with a cross-correlation score (XCorr) above 1.8, 2.5 or 3.5, respectively. 1.5 Da peptide tolerance and 1.0 Da fragment tolerance, two missed cleavage sites, methionine oxidation as variable peptide modification were admitted. A protein was considered as present in the mixture when two or more unique peptides were identified by the previous criteria.

Immunoprecipitations

For immunoprecipitation by magnetic beads (Dynobeads, Invitrogen), MEF cells from 1-2 T-75 cm^2 flasks or 5 mg crude membranes of Raji cells were solubilized in 1 ml precipitation buffer containing 20 mM Tris-HCl, pH 7.4, 1% digitonin, 150 mM NaCl, 5 mM $MgCl_2$ and 1% protease inhibitor mix (Serva) for 1 h on ice. Further steps were performed as described (Demirel et al., 2010). For immunoprecipitations via protein G agarose (Sigma-Aldrich), the lysate of MEF cells was incubated with 30 µg antibodies. 60 µl of protein G agarose were washed twice in buffer containing 20 mM Tris-HCl, pH 7.4, 0.1% digitonin and 150 mM NaCl, added to the sample and incubated for another 1.5 h at 4℃. After four times of washing, bound protein was eluted with 35 µl sample buffer, separated by SDS-PAGE (5–15%), transferred onto nitrocellulose membrane and visualized by immunodetection.

Pulse-chase labeling

Transduced MEFs were seeded with a density of 2–3×10^6 per 10 cm dish. The following day, cells were washed twice with PBS and starved for one hour in cysteine/methionine free DMEM (Invitrogen) containing 3% dialyzed fetal bovine serum (Invitrogen), 2 mM L-glutamine, 100 µg/ml penicillin and 100 µg/ml streptomycin. Subsequently, cells were pulsed for 3 h with 3 ml of starving medium supplemented with ca. 200 µCi [^{35}S]cysteine/methionine (Hartmann Analytics, Braunschweig, Germany) and chased for the indicated time points. Immunoprecipitations were performed as described above except that 750 µl of RIPA (Pierce, Rockford, IL, USA) instead of precipitation buffer was used for solubilization. Eluted proteins were separated on 9% SDS-PAGE and blotted onto nitrocellulose membrane. After electrotransfer, the nitrocellulose membrane was exposed overnight to an imaging plate (BAS-MS, Fujifilm, Dusseldorf, Germany). Signals were detected with a Typhoon phosphorimager (GE Healthcare) and analyzed by ImageQuant analysis software.

Immunofluorescence

Stably transduced and sorted MEF cells grown on poly-D-lysine-coated coverslips were fixed for 30 min with 4% paraformaldehyde in PBS at room temperature, quenched with 50 mM glycine for 10 min and permeabilized with 0.2% saponin for 20 min. In the following steps, all buffers were supplemented with 0.2% saponin. After blocking with 5% bovine serum albumin for 30 min, cells were stained with indicated primary antibodies followed by fluorophor labeled secondary antibody for 1 h at room temperature, respectively. Unbound secondary antibody was removed by washing and cells were subsequently stained with rabbit anti-TAPL directly conjugated with Dylight Alexa 488 (Pierce). Nucleus was visualized by DAPI (Dianova). Samples were mounted in 0.1 M Tris-HCl, pH 8.5, 25% (w/v) glycerol, 10% (w/v) Mowiol (Calbiochem, Darmstadt, Germany). Raji cells were stained as described previously (Demirel et al., 2007). Samples were analyzed with a confocal laser-scanning microscope (LSM 510, Zeiss, Jena, Germany) with a Plan-Apochromat 63× oil immersion objective (numerical aperture, 1.4). In order to reduce blur, improve resolution and reduce background, blind deconvolution with the program Auto Deblur (Bitplane AG, Zurich, Switzerland) was performed.

Transport assay

Non-transduced or transduced MEFs (2.5×10^6 cells) in 50 µl PBS supplemented with 10 mM $MgCl_2$ were semi-permeabilized with 0.0125% saponin for 1 min at room temperature and washed subsequently twice. Transport was started by addition of 5 µM fluorescein-labeled peptide RRYC$^{(\Phi)}$KSTEL (Φ indicates fluorescein coupled via a cysteine residue) in the presence of 10 mM ATP or AMP and 10 mM $MgCl_2$ and stopped after 3 min at 32℃ with 1 ml ice-cold stop buffer (PBS supplemented with 20 mM EDTA). Cells were washed twice with 1 ml stop buffer and lysed with 250 µl PBS containing 1% NP-40 for 10 min at room temperature. Lysed cells were centrifuged and fluorescent peptide in the supernatant was quantified by a fluorescence plate reader ($\lambda_{ex/em}$ 485/520 nm; Polarstar Galaxy, BMG Offenburg, Germany).

Transport in crude membranes was performed as described previously (Demirel et al., 2007). In short, crude membranes (100 µg protein) were incubated in 50 µl PBS supplemented with 2 µM fluorescein-labeled peptide RRYC$^{(\Phi)}$KSTEL and 5 mM $MgCl_2$. Transport was started by the addition of 3 mM ATP or AMP. After 30 min at 32℃, transport was stopped by the addition of 250 µl stop buffer. After 15 min incubation on ice, samples were transferred to microfilter plates preincubated with 0.3% polyethylene imine (MultiScreen plates, Durapore membrane, 1 µm pore size, Millipore). Filters were washed three times with 250 µl ice-cold stop buffer. Subsequently, the filters were incubated with 250 µl elution buffer (PBS, 1% SDS) for 10 min. Fluorescent peptides were quantified with a fluorescence plate reader.

Acknowledgements

We thank Christine Le Gal for preparation of the manuscript.

Funding

This work was supported by Studienstiftung des Deutschen Volkes (Ö.D.) and by the German Research foundation [grant number SFB 807 to R.A. and I.J.; GRK1459 to P.S.] and the Centers of Excellence “Macromolecular complexes” to R.A. and “Inflammation at Interfaces” to P.S.

Supplementary material available online at
http://jcs.biologists.org/lookup/suppl/doi:10.1242/jcs.087346/-/DC1

References

Andrejewski, N., Punnonen, E. L., Guhde, G., Tanaka, Y., Lüllmann-Rauch, R., Hartmann, D., von Figura, K. and Saftig, P. (1999). Normal lysosomal morphology and function in LAMP-1-deficient mice. *J. Biol. Chem.* **274**, 12692-12701.

Aniento, F., Roche, E., Cuervo, A. M. and Knecht, E. (1993). Uptake and degradation of glyceraldehyde-3-phosphate dehydrogenase by rat liver lysosomes. *J. Biol. Chem.* **268**, 10463-10470.

Bagshaw, R. D., Mahuran, D. J. and Callahan, J. W. (2005). A proteomic analysis of lysosomal integral membrane proteins reveals the diverse composition of the organelle. *Mol. Cell. Proteomics* **4**, 133-143.

Ballabio, A. and Gieselmann, V. (2009). Lysosomal disorders: from storage to cellular damage. *Biochim. Biophys. Acta* **1793**, 684-696.

Bonifacino, J. S. and Traub, L. M. (2003). Signals for sorting of transmembrane proteins to endosomes and lysosomes. *Annu. Rev. Biochem.* **72**, 395-447.

Chan, K. W., Zhang, H. and Logothetis, D. E. (2003). N-terminal transmembrane domain of the SUR controls trafficking and gating of Kir6 channel subunits. *EMBO J.* **22**, 3833-3843.

Cuervo, A. M. and Dice, J. F. (2000). Unique properties of lamp2a compared to other lamp2 isoforms. *J. Cell Sci.* **113**, 4441-4450.

Demirel, Ö., Waibler, Z., Kalinke, U., Grünebach, F., Appel, S., Brossart, P., Hasilik, A., Tampé, R. and Abele, R. (2007). Identification of a lysosomal peptide transport system induced during dendritic cell development. *J. Biol. Chem.* **282**, 37836-37843.

Demirel, Ö., Bangert, I., Tampé, R. and Abele, R. (2010). Tuning the cellular trafficking of the lysosomal peptide transporter TAPL by its N-terminal domain. *Traffic* **11**, 383-393.

Escola, J. M., Kleijmeer, M. J., Stoorvogel, W., Griffith, J. M., Yoshie, O. and Geuze, H. J. (1998). Selective enrichment of tetraspan proteins on the internal vesicles of multivesicular endosomes and on exosomes secreted by human B-lymphocytes. *J. Biol. Chem.* **273**, 20121-20127.

Eskelinen, E. L., Illert, A. L., Tanaka, Y., Schwarzmann, G., Blanz, J., Von Figura, K. and Saftig, P. (2002). Role of LAMP-2 in lysosome biogenesis and autophagy. *Mol. Biol. Cell* **13**, 3355-3368.

Eskelinen, E. L., Schmidt, C. K., Neu, S., Willenborg, M., Fuertes, G., Salvador, N., Tanaka, Y., Lüllmann-Rauch, R., Hartmann, D., Heeren, J. et al. (2004). Disturbed cholesterol traffic but normal proteolytic function in LAMP-1/LAMP-2 double-deficient fibroblasts. *Mol. Biol. Cell* **15**, 3132-3145.

Eskelinen, E. L., Cuervo, A. M., Taylor, M. R., Nishino, I., Blum, J. S., Dice, J. F., Sandoval, I. V., Lippincott-Schwartz, J., August, J. T. and Saftig, P. (2005). Unifying nomenclature for the isoforms of the lysosomal membrane protein LAMP-2. *Traffic* **6**, 1058-1061.

Furuta, K., Yang, X. L., Chen, J. S., Hamilton, S. R. and August, J. T. (1999). Differential expression of the lysosome-associated membrane proteins in normal human tissues. *Arch. Biochem. Biophys.* **365**, 75-82.

Gompf, S., Zutz, A., Hofacker, M., Haase, W., van der Does, C. and Tampé, R. (2007). Switching of the homooligomeric ATP-binding cassette transport complex MDL1 from post-translational mitochondrial import to endoplasmic reticulum insertion. *FEBS J.* **274**, 5298-5310.

Gough, N. R., Hatem, C. L. and Fambrough, D. M. (1995). The family of LAMP-2 proteins arises by alternative splicing from a single gene: characterization of the avian LAMP-2 gene and identification of mammalian homologs of LAMP-2b and LAMP-2c. *DNA Cell Biol.* **14**, 863-867.

Hatem, C. L., Gough, N. R. and Fambrough, D. M. (1995). Multiple mRNAs encode the avian lysosomal membrane protein LAMP-2, resulting in alternative transmembrane and cytoplasmic domains. *J. Cell Sci.* **108**, 2093-2100.

Isaac, E. L., Karageorgos, L. E., Brooks, D. A., Hopwood, J. J. and Meikle, P. J. (2000). Regulation of the lysosome-associated membrane protein in a sucrose model of lysosomal storage. *Exp. Cell Res.* **254**, 204-209.

Kamakura, A., Fujimoto, Y., Motohashi, Y., Ohashi, K., Ohashi-Kobayashi, A. and Maeda, M. (2008). Functional dissection of transmembrane domains of human TAP-like (ABCB9). *Biochem. Biophys. Res. Commun.* **377**, 847-851.

Kobayashi, A., Hori, S., Suita, N. and Maeda, M. (2003). Gene organization of human transporter associated with antigen processing-like (TAPL, ABCB9): analysis of alternative splicing variants and promoter activity. *Biochem. Biophys. Res. Commun.* **309**, 815-822.

Koch, J., Guntrum, R., Heintke, S., Kyritsis, C. and Tampé, R. (2004). Functional dissection of the transmembrane domains of the transporter associated with antigen processing (TAP). *J. Biol. Chem.* **279**, 10142-10147.

Kyritsis, C., Gorbulev, S., Hutschenreiter, S., Pawlitschko, K., Abele, R. and Tampé, R. (2001). Molecular mechanism and structural aspects of transporter associated with antigen processing inhibition by the cytomegalovirus protein US6. *J. Biol. Chem.* **276**, 48031-48039.

Lehner, P. J., Surman, M. J. and Cresswell, P. (1998). Soluble tapasin restores MHC class I expression and function in the tapasin-negative cell line. 220. *Immunity* **8**, 221-231.

Leveson-Gower, D. B., Michnick, S. W. and Ling, V. (2004). Detection of TAP family dimerizations by an in vivo assay in mammalian cells. *Biochemistry* **43**, 14257-14264.

Lotteau, V., Teyton, L., Peleraux, A., Nilsson, T., Karlsson, L., Schmid, S. L., Quaranta, V. and Peterson, P. A. (1990). Intracellular transport of class II MHC molecules directed by invariant chain. *Nature* **348**, 600-605.

Lübke, T., Lobel, P. and Sleat, D. E. (2009). Proteomics of the lysosome. *Biochim. Biophys. Acta* **1793**, 625-635.

Neumann, L. and Tampé, R. (1999). Kinetic analysis of peptide binding to the TAP transport complex: evidence for structural rearrangements induced by substrate binding. *J. Mol. Biol.* **294**, 1203-1213.

Nishino, I., Fu, J., Tanji, K., Yamada, T., Shimojo, S., Koori, T., Mora, M., Riggs, J. E., Oh, S. J., Koga, Y. et al. (2000). Primary LAMP-2 deficiency causes X-linked vacuolar cardiomyopathy and myopathy (Danon disease). *Nature* **406**, 906-910.

Piper, R. C. and Katzmann, D. J. (2007). Biogenesis and function of multivesicular bodies. *Annu. Rev. Cell Dev. Biol.* **23**, 519-547.

Radons, J., Faber, V., Buhrmester, H., Völker, W., Horejsí, V. and Hasilik, A. (1992). Stimulation of the biosynthesis of lactosamine repeats in glycoproteins in differentiating U937 cells and its suppression in the presence of NH4Cl. *Eur. J. Cell Biol.* **57**, 184-192.

Reczek, D., Schwake, M., Schröder, J., Hughes, H., Blanz, J., Jin, X., Brondyk, W., Van Patten, S., Edmunds, T. and Saftig, P. (2007). LIMP-2 is a receptor for lysosomal mannose-6-phosphate-independent targeting of beta-glucocerebrosidase. *Cell* **131**, 770-783.

Reggiori, F. and Pelham, H. R. (2001). Sorting of proteins into multivesicular bodies: ubiquitin-dependent and -independent targeting. *EMBO J.* **20**, 5176-5186.

Saftig, P. (2005). *Lysosomes*. Georgetown, Texas: Springer Science+Buisness Media, Inc.

Saftig, P. and Klumperman, J. (2009). Lysosome biogenesis and lysosomal membrane proteins: trafficking meets function. *Nat. Rev. Mol. Cell Biol.* **10**, 623-635.

Schröder, B., Wrocklage, C., Pan, C., Jäger, R., Kösters, B., Schäfer, H., Elsässer, H. P., Mann, M. and Hasilik, A. (2007). Integral and associated lysosomal membrane proteins. *Traffic* **8**, 1676-1686.

Tanaka, Y., Guhde, G., Suter, A., Eskelinen, E. L., Hartmann, D., Lüllmann-Rauch, R., Janssen, P. M., Blanz, J., von Figura, K. and Saftig, P. (2000). Accumulation of autophagic vacuoles and cardiomyopathy in LAMP-2-deficient mice. *Nature* **406**, 902-906.

Washburn, M. P., Wolters, D. and Yates, J. R., 3rd (2001). Large-scale analysis of the yeast proteome by multidimensional protein identification technology. *Nat. Biotechnol.* **19**, 242-247.

Wolters, J. C., Abele, R. and Tampé, R. (2005). Selective and ATP-dependent translocation of peptides by the homodimeric ATP binding cassette transporter TAP-like (ABCB9). *J. Biol. Chem.* **280**, 23631-23636.

Zhang, F., Zhang, W., Liu, L., Fisher, C. L., Hui, D., Childs, S., Dorovini-Zis, K. and Ling, V. (2000). Characterization of ABCB9, an ATP binding cassette protein associated with lysosomes. *J. Biol. Chem.* **275**, 23287-23294.

Zhao, C., Haase, W., Tampé, R. and Abele, R. (2008). Peptide specificity and lipid activation of the lysosomal transport complex ABCB9 (TAPL). *J. Biol. Chem.* **283**, 17083-17091.